D-A107 538 ENVIRONMENTAL FAILURE OF ADHESIVE BONDING IN COMPOSITES.(U)(FINAL REPT.) / E. H. ANDREWS, ET AL. EUROPEAN RESEARCH OFFICE, LONDON (ENGLAND). MAY 81

UNCLASSIFIED

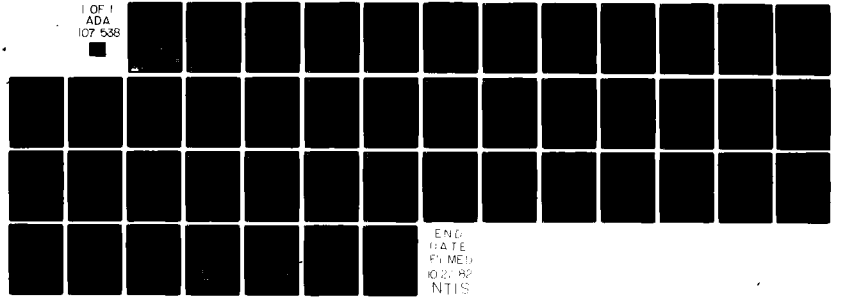

ENVIRONMENTAL FAILURE OF ADHESIVE BONDING IN COMPOSITES

E. H. Andrews, et al

European Research Office
London, England

May 81

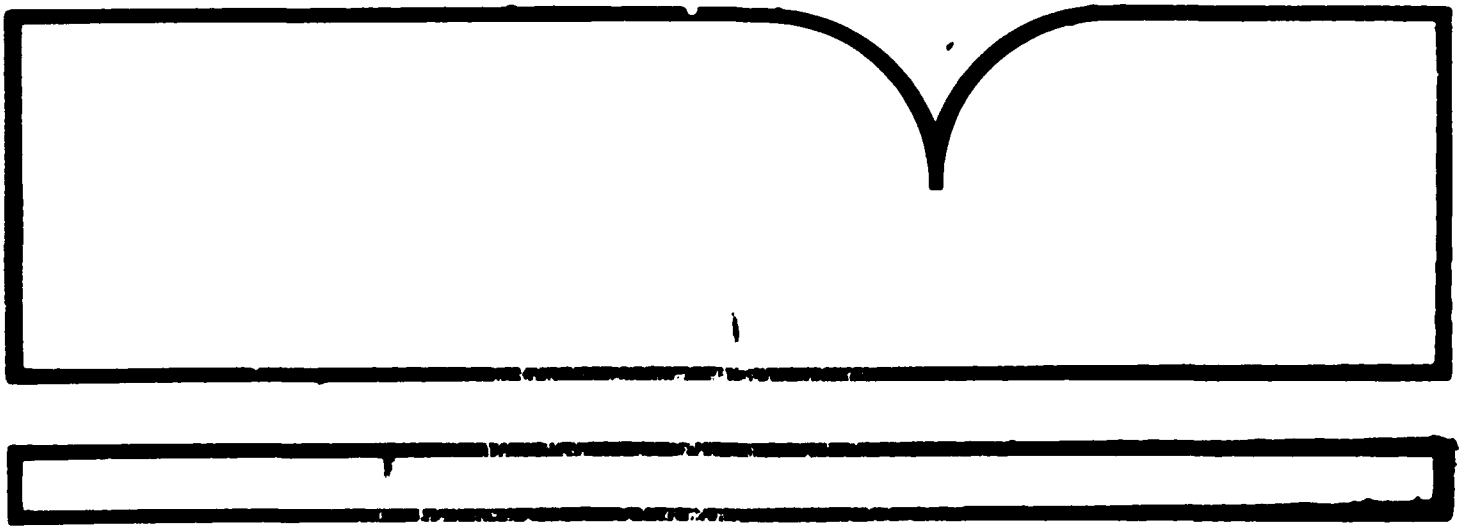

FINAL REPORT

ENVIRONMENTAL FAILURE OF ADHESIVE BONDING IN COMPOSITES

by

E.H. Andrews, Ho Ping Sheng, H.A. Majid
and C. Vlachos

May 1981

EUROPEAN RESEARCH OFFICE

UNITED STATES ARMY
London England

GRANT NO. DAERO/78/G/118

Department of Materials
Queen Mary College, London

ABSTRACT

A recently developed fracture mechanics test (the A-S test), which involves pressurisation of an enclosed circular flaw, has been used to investigate the adhesion of two epoxy resins (Shell Epikote 828 and 3 M's SP 250) to glass. Specimens were tested after various times of immersion in water at 80°C and the adhesive failure energy θ determined. The effects of adding silane coupling agents to the epoxy resin, and the influence of water pH were particularly studied.

The theory of generalized fracture mechanics is used to derive, from θ, an intrinsic failure energy θ_o which is the energy to break unit area of interatomic bonds across the interface. The decrease of θ_o with time follows first order reaction kinetics, with a rate constant controlled by the type and concentration of coupling agent as well as by the pH of the aqueous environment. The results are interpreted in terms of the chemical hydrolysis of interfacial bonds.

Part I

ENVIRONMENTAL FAILURE OF ADHESIVE BONDS BETWEEN GLASS AND EPIKOTE 828

1. INTRODUCTION

The adhesive bonding of polymeric resins to glass assumes major importance in the glass reinforced composite materials used increasingly in structural and aerospace application. Good bonding is essential, not only for the structural integrity of the composite but also to ensure adequate stress transfer from the polymer matrix to the reinforcing fibres.

Epoxy resins are capable of providing an excellent adhesive bond to glass, but the adhesion deteriorates progressively in the presence of moisture. This process is slowed, but not eliminated, if the glass fibres are 'sized' with coupling agents to promote adhesion and durability.

A number of studies have been carried out on the deterioration of glass-to-epoxy bonds in water [Kaelble and Dynes, 1977, Comyn et al 1979, Sargent and Ashbee 1980], but quantitative conclusions are not easy to obtain because of the complex stress patterns produced by differential thermal contraction between the resin and the glass as the system cools from its curing temperature. Furthermore, conventional adhesion tests measure parameters which are only indirectly related to the actual interatomic bonding energies at the interface [Andrews and Kinloch 1973]. It is therefore difficult to monitor changes in these bonding energies with exposure to water or with the addition of coupling agents.

Many of these problems can be overcome by combining the experimental technique of Andrews and Stevenson [1978] with the analytical method of Generalized Fracture Mechanics (GFM) [Andrews 1974]. Using this approach Andrews and Stevenson [1980] studied the deterioration in water of epoxy resin-to-titanium bonds and derived the interfacial bonding energy, θ_o, as a function of time -

of immersion and environmental pH. They explained their results in terms of the chemical hydrolysis of interfacial bonds, and their conclusions will be considered further in the discussion section of this paper.

The work described here is similar to that reported by Andrews and Stevenson on epoxy-titanium systems except that 'Pyrex' glass was used as a substrate and silane coupling agents were incorporated into the resin in various proportions to determine their effects.

2. MATERIALS

The epoxy resin used throughout this work was "Shell Epikote 828", a diglicidyl ether of bis-phenol A of molecular mass ∿ 370. The hardener was "Shell Epikure 114", a blend of two cycloaliphatic amines with added benzyl alcohol as an accelerator. These components were mixed in the stoichiometric mass ratio of 5:2, cast and allowed to gel for 24 hours at room temperature, before post curing at 130°C for 1.5 h. Specimens were cooled at 30°C/h. The resulting resin has a glass transition temperature of 72°C.

Three different silane coupling agents were employed (supplied by Union Carbide Limited) as follows:

A 1120 N-β-aminoethyl-γ-aminopropyl trimethoxy silane.

$H_2NCH_2CH_2NHCH_2CH_2CH_2Si(OCH_3)_3$

A 187 γ-glycidoxypropyl trimethoxysilane

$CH_2\text{-}CHCH_2OCH_2CH_2CH_2Si(OCH_3)_3$ (epoxide ring: CH_2–CH–O)

A 1100 γ-aminopropyltriethoxysilane

$H_2NCH_2CH_2CH_2Si(OC_2H_5)_3$

The silanes were added to the epoxy resin, before casting, in various weight proportions as follows:

TABLE I

	0.05%	0.1%	0.2%	0.5%	0.7%	1.0%
A 1120	s,f	s,f	s	s		
A 187	s,f	s,f	s	s	s	s
A 1100						f

Note: s used to determine time to complete adhesive failure
f used in fracture studies

The coupling agents were added to the bulk resin to give quantitative control of silane concentration. If the more normal method of applying the silane to the glass surface had been adopted, the amount applied would have been difficult to ascertain with any precision. Moreover, solubility of silane in the resin would cause migration of such a surface coating into the epoxy during the curing process and give rise to even further uncertainties concerning the silane concentration at the bonded interface. Although we cannot rule out migration of silane to the interface from solution in the resin, there would be no severe concentration gradients to drive such migration and it can be assumed to a first approximation that the coupling agent remains uniformly dispersed in the cured resin.

The glass employed throughout was 'Pyrex' sheet glass of the following nominal composition:- SiO_2 80.6%; B_2O_3 12.6%; Na_2O 4.2%; Al_2O_3 2.2%

Square 'coupons' of the glass, measuring 5 x 5 cm, were cut from sheet of thickness 3 mm or 6 mm, and drilled centrally with a 6 mm diameter hole using a diamond impregnated drill. Their surfaces were cleaned by washing with water and acetone and dried.

3. EXPERIMENTAL METHOD

The basic specimen employed is illustrated in Fig. 1 and consist of the 'coupon' described above, on to which is cast a squat cylindrical block of epoxy resin approximately 30 mm in radius and 8 ∿ 11 mm in height.

The drilled central hole is covered by a thin circular disc of PTFE before the resin is cast, the disc thus creating a non-adhering region which acts as an inclosed circular crack which can be pressurized internally through the hole. This system provides a totally plane-strain fracture mechanics test in which, moreover, stresses due to differential thermal contraction between the resin and the glass cannot assist crack propagation as long as the latter is interfacial. These and other advantages of the test have been discussed previously [Andrews and Stevenson 1978].

Although the specimens shown in Fig. 1(a) proved highly suitable for epoxy to metal bonding, they failed in the case of glass substrates, where the thermal contraction stresses already referred to are sufficient to produce spontaneous cone fractures in the glass. A modification was therefore introduced as shown in Fig. 1(b) in which a thin metal annulus (a steel 'washer') is first cemented to the glass using the same epoxy resin as is to be cast. The cast resin cylinder is then positioned so that its outer edges (where the shear stress due to contraction is a maximum) are carried upon the metal annulus rather than the glass. Such specimens were found to retain their integrity under all conditions used in this work. However, the epoxy resin employed in these studies had a glass transition temperature of 72°C. Resins with significantly higher T_g's (in the region of 140°C) still cause cracking of the glass even with the arrangement of Fig.1(b) unless very thin layers of resin are used.

The cohesive and adhesive fracture energies (critical energy release rates) for such a specimen are given respectively by the following equations [Andrews and Stevenson 1978].

Cohesive:- $2\mathcal{J} = P_c^2 c/E[f_1(h/c)]$

Adhesive:- $\theta = P_c^2 c/E[f_2(h/c)]$

where P_c is the critical pressure
c is the circular flaw radius
h is the resin cyclinder height
ν is poisson's ratio
E is the Young's modulus of the resin

and

$$f_1 = \frac{1}{1-\nu^2}\left\{\frac{3}{32}\left[\left(\frac{c}{h}\right)^3 + \left(\frac{c}{h}\right)\frac{4}{1-\nu}\right] + \frac{1}{\pi}\right\}^{-1}$$

$$f_2 = \frac{1}{1-\nu^2}\left\{\frac{3}{32}\left[\left(\frac{c}{h}\right)^3 + \left(\frac{c}{h}\right)\frac{4}{1-\nu}\right] + \frac{2}{\pi}\right\}^{-1}$$

The crack velocity is an important variable in these studies [Andrews and King 1976, Andrews and Stevenson 1980] and this was measured by a 'Hispeed' cinematographic camera used in a streak mode as has been fully described elsewhere [Andrews and Stevenson 1978].

Specimens were tested, both dry and after immersion in water at 80°C for various times ranging from 100 to 5000 h. All fracture tests were carried out at room temperature (20 ± 2°C), critical pressure and crack velocity being recorded for each specimen. Fracture energy determinations were not, however, carried out for all proportions of coupling agent, but only those indicated by the letter f in Table I. The mixes marked s in the Table were tested for the onset of completely adhesive failure by immersing specimens for a range of times and testing without crack velocity determination. The minimum time of immersion at 80°C required to produce totally adhesive failure was then deduced by inspection of the failed interface. This time will be designated t_a.

4. RESULTS AND DISCUSSION

4.1 Crack velocity dependence

The basic data obtained from the fracture tests take the form shown in Fig. 2 and 3 where cohesive ($2\mathcal{J}$) or adhesive (ϑ) failure energy is plotted as ordinate against crack velocity $\dot{c}$ as abcissa for various times of immersion in water at 80°C and 7.8 pH. Figure 2 shows data for resin containing no coupling agent whilst Fig. 3 refers to a mix containing 0.1% of A 187 silane. Several things are immediately apparent. Firstly, the complex velocity dependence is the same in character for both cohesive and adhesive failure. This is a prediction of the generalized theory of fracture mechanics as we shall see below. Secondly, immersion causes a steady overall decrease in failure energy without any marked change in the velocity dependence. This again is expected from generalized theory. Thirdly, the resin incorporating coupling agent suffers a much slower degradation of interfacial strength. Although there is a factor of two difference in the vertical scales of Figs. 2 and 3, it is clear that the system containing coupling agent has deteriorated after 863 h to about the same degree as obtained after 40 h with unprotected resin. Fourthly, a shift in the peak of the curve along the $\dot{c}$ axis is observed after long periods of immerison, from about 30 m/s for dry material to about 42 m/s for long immersion times. An identical shift was previously observed for the same epoxy resin bonded to titanium metal [Andrews and Stevenson 1980] and is attributable to plasticization of the resin by water. At 80°C the shift occurs during the first 100 h and once it has happened no further movement of the curve takes place. It was also found in the epoxy-titanium system that the peak of the curve increased in height as a result of plasticization, and this fact will have to be taken into account in the

analysis of the results. Data for all resin mixes can be displayed in the same form as Figs. 2 and 3.

4.2 Analysis of data

According to generalized fracture mechanics [Andrews 1974] the cohesive and adhesive failure energies can be expressed in the form:

$$\text{Cohesive} \quad 2\mathcal{J} = 2\mathcal{J}_o \, \phi \, (\dot{c}, T, \varepsilon_o) \qquad (1)$$

$$\text{Adhesive} \quad \theta = \theta_o \, \phi \, (\dot{c}, T, \varepsilon_o) \qquad (2)$$

where $2\mathcal{J}$, θ are the cohesive and adhesive failure energies per unit area respectively, the cohesive term being resolvable into two equal parts because there are two identical surfaces created by crack propagation; $2\mathcal{J}_o$ and θ_o are the energies required to fracture unit area of inter-atomic bonds across the fracture plane in cohesive and adhesive failure respectively; ϕ is the loss function for the epoxy resin, being dependent upon crack velocity, temperature and overall strain level. The last of these dependencies can usually be ignored.

The $\dot{c}$ dependence of $2\mathcal{J}$ and θ is thus seen to lie in the loss function which appears equally in the equations for cohesive and adhesive failure. This is why the curves in Figs. 1 and 2 are similar in shape for both modes of failure. Furthermore, it is ϕ which changes due to plasticization of the bulk epoxy resin. Taking logarithms:

$$\log 2\mathcal{J} = \log 2\mathcal{J}_o + \log \phi \qquad (3)$$

$$\log \theta = \log \theta_o + \log \phi \qquad (4)$$

Since neither $\mathcal{J}_o$ and θ_o should be functions of rate, this implies that plots of log $2\mathcal{J}$ or log θ against crack velocity (or its logarithm) should be superimposable by vertical shift. This was found to be the case for the epoxy-titanium system [Andrews and Stevenson 1980].

If ϕ were constant with time of immersion, the vertical shift required to superimpose adhesive failure curves on to the cohesive failure curve would equal log $(2\mathcal{J}_o/\theta_o)$. Since an absolute value for $2\mathcal{J}_o$ of 2.59 Jm^{-2} is available for this resin [King and Andrews 1978], it would then be possible to deduce an absolute value for θ_o after any time or condition of immersion.

Unfortunately, ϕ is subject to change as the resin becomes progressively plasticized by water over the first 100 h of immersion, after which its behaviour stabilises. This means that absolute θ_o values cannot be deduced immediately, although relative values will be correct after the first 100 h. This problem can be overcome, as we shall see presently. Meanwhile we make the temporary assumption that ϕ is changed by plasticization is such a manner that its value is magnified by a quantity a after 100 h and thereafter remains constant.

$$\phi \text{ (plasticized)} = a\,\phi \text{ (dry)} \qquad (5)$$

then,

$$\log 2\mathcal{J} = \log 2\mathcal{J}_o + \log \phi \qquad (6)$$

$$\log \theta = \log \theta_o + \log \phi + \log a \qquad (7)$$

and the vertical shift required to superimpose log θ data upon log $2\mathcal{J}$ data is

$$\log (2\mathcal{J}_o/a\theta_o) \equiv \log q \qquad (8)$$

Using the known value for $\mathcal{J}_o$, we may immediately deduce a value for a θ_o after any time of immersion.

Following these procedures, results may be obtained of the kind displayed in Figs. 4 to 7. Figure 4 is a 'master curve' obtained by vertical

superposition of the logarithmic data for the unprotected resin after various times of immersion as indicated by the symbols. This figure also contains the master curve for fully plasticized resin obtained in the work on epoxy-titanium bonds. It is clear that the time scale over which the unprotected resin debonds from glass is too short for plasticization of the bulk resin to be completed. In Fig. 5 is a similar master curve for resin containing A1120 coupling agent in various proportions and various immersion times exceeding 100 h. In this case the match with the epoxy-titanium master curve is much closer. The shape of the master curve does not appear to depend upon the coupling agent employed, its concentration, the time of immersion (after the first 100 h), or the pH of the immersion medium.

4.3 Derivation of reaction rate constants

In Fig. 6 comprehensive results for log a θ_o are plotted against time of immersion for a range of coupling agents, concentrations and pH values. As explained previously [Andrews and Stevenson 1980] a linear dependence of log θ_o upon time is characteristic of a first order chemical reaction, the negative slope of such a plot being what we shall call the overall rate constant, k':

$$k' = [A][B]\, k_{80}/2.303 \qquad (9)$$

where [A] and [B] are respectively the concentrations of hydrolysable bonds and water at the interface, and k_{80} is the true rate constant at 80°C. For comparative purposes it is sufficient to talk in terms of k' since the water concentration should be sensibly constant at its equilibrium uptake value (some 8% at 80°C). The value of [A] will be discussed presently.

The slopes k' are, of course, unaffected by the value of a except for times under 100 h immersion. The fact that, within experimental error, all lines converge to a single intercept at t = 0 is also unaffected by the value of a. Only the absolute value of this intercept is affected by the arbitrary constant.

4.4 Absolute Values of θ_o

In order to establish the absolute values of θ_o (and thus of θ_o at zero time), we make use of the idea that a transition from cohesive to adhesive failure will occur when $2\gamma_o = \theta_o$. Thus, for unimmersed specimens $\theta_o > 2\gamma_o$ and fracture is always cohesive. As θ_o is progressively reduced by hydrolysis of the interfacial bonds, there comes a time when it falls below $2\gamma_o$ and the interface becomes weaker than the bulk resin. This assumes, of course, that $2\gamma_o$ itself is not significantly affected by hydrolysis.

The time required to produce complete interfacial or adhesive failure was determined for a wide range of resin compositions and conditions of exposure and will be denoted t_a. The time t_b at which θ_o falls to the value $2\gamma_o$ will be less than t_a because t_a includes the time required for water to diffuse in sufficient concentration across the whole interfacial area. This time is known to be approximately 100 h [Andrews and Stevenson 1980]. Water uptake measurements have also established that the diffusion coefficient of water in resin is not significantly affected by silane content. We may therefore set,

$$t_b = t_a - 100 \qquad (10)$$

The absolute values of θ_o in Fig. 6 may now be established by shifting the entire set of data vertically until each line of slope k' crosses the horizontal line $\theta_o = 2\gamma_o$ at the time t_b. Since t_b varies with coupling agent type and content, and also with pH, and since all the data must shift together, we have to achieve a simultaneous, multi-point fit.

The result is shown in Fig. 7 where the lines from Fig. 6, with experimental points omitted for clarity are shown shifted simultaneously to give the best overall fit with the t_b data. The agreement is good, providing considerable confidence in the assumptions entailed in constructing this plot. There is a tendency for t_b to be too large for the lowest k' and too small for the highest k' data and although these deviations are hardly greater than experimental error, their progressive character probably indicates that our assumptions are not completely accurate. The observed deviations would arise, for example, if the parameter $\underline{a}$ were not strictly constant at $t > 100$ h, i.e. if ϕ increased slowly with long times of immersion, perhaps as a result of bulk hydrolysis and a consequent loosening of the molecular network. A similar effect would be produced if $2\gamma_o$ increased with prolonged immersion, and this could also occur as a result of a looser network (larger M_c). However, the effect appears to be relatively small and will be ignored in drawing our quantitative conclusions.

4.5 Dry value of θ_o

All the data, regardless of resin composition and pH, converge within experimental error to a single value of θ_o at $t = 0$, i.e. for the dry reisn/glass bond. This point is, of course, experimentally inaccessible since without immersion all specimens fracture cohesively and no information on the strength of the interface can be deduced (except that $\theta_o > 2\gamma_o$). The extrapolation of data for specimens at different pH values should, of course give a single intercept, since all these joints are identical before immersion. Nevertheless, the fact that they do converge to a single value of θ_o is strong evidence that this value can be taken as the actual interfacial bonding energy of the freshly made interface. The point of major interest is that even specimens differing widely in silane content also yield the same θ_o (dry).

The value in question is 7.25 Jm^{-2}, some twenty-four times larger than the expected Van der Waals interaction energy for such a system [Andrews and King 1976]. This indicates that some at least of the interfacial bonds are primary, but a precise proportion is more difficult to specify. A figure of 25 to 50% of primary bonds would appear to be reasonable, based on the relative dissociation energies or primary and secondary bonds. However, as Ahagon and Gent [1975] point out in their work on elastomeric adhesives bonded to glass, a single primary interfacial bond may require many times the energy for rupture of a single C-C bond because it is attached to a length of network chain. According to the theory of Lake and Thomas [1967], which is well supported experimentally, the apparent dissociation energy of a single chemical bond in a network chain is very large because of the energy stored in neighbouring bonds which do not undergo fracture. This apparent dissociation energy would be of the order of $2\mathcal{J}_o$, i.e. 2.59 Jm^{-2}, when referred to unit area. For the resin employed, the number of network chains crossing unit area is of the order of 3.8×10^{18} m^{-2}, some ten times smaller than the atomic packing density [King and Andrews 1978]. Taking these factors together, the magnitude of $\mathcal{J}_o$ (dry) can be explained if between 30% and 60% of all interfacial bonds are primary in nature. The lower figure applies if all network chains terminating on the surface are chemically bonded to it and if the cross-link density is the same at the interface as in the bulk. The higher figure would apply if the network chain effect were totally suppressed by chain immobilisation at the interface.

The most surprising feature of the $\mathcal{J}_o$ (dry) result is that it appears insensitive to the quantity of silane added to the resin, even though the rate constant for hydrolysis is greatly enhanced by the coupling agent.

The obvious explanation is that, with the addition of silane, the total number of interfacial primary bonds remains the same but that the type of bond changes. That is, primary bonds which are established in the absence of silane (presumably R-C-O-Si) are progressively replaced by different bonds (presumably R-Si-O-Si) until the interface is saturated with silane-related bonds. Under dry conditions these two types of bond would have very similar strength, but under hydrolytic action the silane-related bond would degrade much more slowly.

4.6 Variation of rate constants

Finally, we may seek information on the interfacial hydrolysis process by examining the variation of k' with the type and concentration of coupling agent and with pH.

Since all data extrapolate to a single θ_o (dry) value, there is a simple relationship between k' and t_a, namely:

$$k' = [\theta_o (dry) - 2J_o]/[t_a - 100] \qquad (11)$$

Extensive measurements were made of t_a and these allow k' to be plotted as a function of both pH and silane concentration. Such results are shown in Figs. 8 and 9.

Figures 8 shows k' as a function of pH for resin containing no silane. Hydrolytic activity is at a minimum for neutral pH, rising dramatically for both acidic and alkaline conditions. This is in distinct contrast to the results obtained for the same resin using titanium as a substrate [Andrews and Stevenson 1980]. There, acidic conditions accelerated the hydrolysis reaction but alkalinity retarded it. This difference constitutes strong circumstantial evidence that the hydrolysing bonds are genuinely interfacial. If the locus of hydrolysis were the bulk

resin, no difference should be observed between glass and metal substrates. Figure 8 also includes results for resin containing 0.05% of silane A 187. These data are similar to those for unprotected resin except that k' is now smaller at all pH values. Once again, however, neutral pH gives the lowest rate of hydrolysis, and k' rises dramatically for both acidic and alkaline conditions. It should be added that at very high alkaline pH, dissolution of the glass surface is observed and the increase of k' above neutral pH (not observed with T_i substrates) may be due to chemical attack upon the glass rather than the interfacial bonds as such.

The variation of k' with silane concentration is shown in Fig. 9 for silanes A 187 and A 1120. There is an almost linear decrease of k' with concentration up to 0.05% w/w but at concentrations as low as 0.1% saturation is beginning to occur. Although k' continues to fall slowly, saturation is largely achieved at concentrations of 0.5% for both silanes.

We have no information on the likely migration of silane from the epoxy to the interface during curing. It is clear that some such migration occurs since an interfacial concentration of 0.1% could have no dramatic quantitative influence upon the bonding there. However, at 0.1% bulk concentration it would only need 10% of the silane from a layer of resin 0.1 mm thick adjacent to the surface, to form an interfacial layer 10 nm thick. This suggests that ample coupling agent is avilable at the interface to promote the formation of silane-related bonding there, and indeed to provide a polymerised layer of silane between the glass and the bulk resin.

Part II

ENVIRONMENTAL FAILURE OF ADHESIVE BONDS BETWEEN GLASS AND SP 250 EPOXY RESIN

1. INTRODUCTION

The high degree of success obtained using Epikote resin and described in Part I of this report was not repeated with the less tractable SP 250 resin (3 M's Corporation). This situation is due to the higher glass transition temperature of SP 250 which results in much larger interfacial stresses between resin and glass when cast specimens are cooled from T_g to room temperature. Using Epikote 828 (T_g approximately 72°C), it was possible to prevent cone fracture of the glass arising from these stresses by interposing a steel annulus as described in Part I. This device was not effective with SP 250 resin ($T_g \sim 120°$), and cone fracture still ensued.

The only method which proved successful with SP 250 was a 'thin sandwich' arrangement described below (and shown in Fig. 10) in which a thin layer of epoxy resin was sandwiched between glass sheets. Provided the layer of epoxy was less than about 3 mm thick, specimens of this kind remained intact and could be tested in the usual way.

This specimen, however, gave rise to problems of a different kind. Since the crack path length in the resin is so short, it proved impossible to obtain a photographic record of propagation and thus measure crack velocity. An ultrasonic method of measuring crack velocity is under consideration but this technique is in a very early stage of development and is not yet available for use.

The inability to measure crack velocity in thin sandwich specimens is, of course, serious since Part I demonstrates the extreme sensitivity of fracture energy (both cohesive and adhesive) to this quantity.

The method adopted to circumvent this problem was to measure critical pressure (and thus $2\mathcal{J}$ or θ) for a large number of specimens, which gave the expected spread of results due to random velocity variation. However, the upper and lower limits to this spread of data proved to be well defined, as would be expected from the data in Part I. We would also expect from Part I that the width of the band of data would not vary significantly as the interfacial bond deteriorated, but that the data would shift uniformly to lower $2\mathcal{J}$ or θ values. This concept is shown schematically in Fig. 11. Whilst not resolving the velocity dependence of the loss function Φ, this approach does in principle provide information on the change of θ_o with time.

2. MATERIALS AND EXPERIMENTAL DETAILS

SP 250 is a two component epoxy resin supplied by the 3 M's Corporation. The catalyst system is a mixture of an unspecified accelerator and dicyandiamid $(NH_2)_2C = N - C \equiv N$ in the form of a crystalline powder. The resin was heated to 80°C, mixed thoroughly and batched in small glass containers for subsequent use, being stored at - 10°C.

Mixes were prepared for casting by heating to 88°C and adding 12.83 parts by weight of catalyst to every 100 parts of resin (giving 11.37% by weight of catalyst, containing 7.54% of dicyandiamid and 3.83% of an accelerator). The mix was homogenized for 5 to 10 minutes using a 'lightning' mixer.

Although the recommended curing conditions is simply 2 h at 127°C, this was found to cause serious foaming of the resin in our free-cast specimens. It was therefore necessary to adopt a more gentle cure cycle as follows:

a) Leave cast specimens at room temperature for 24 h.
b) Heat to 95°C and hold for 2 h at this temperature.
c) Heat at 3°C/min. to 127°C and hold for 2 h.
d) Cool at 3°C/min.

It is appreciated that varying the cure cycle may alter the chemistry of the reaction and modify the adhesive properties.

Two types of glass were employed, namely 'Pyrex' glass and an ordinary soda-lime glass. The specimens employed is shown in Fig. 10. It consists of a 5 cm x 5 cm square, 6 mm thick glass base plate, drilled with an access hole as described in Part I; a PTFE disc placed over the access hole as before; a small drop of resin placed on the PTFE disc and spread into a uniform thin film by placing on top of it the upper glass sheet (1 mm or 3 mm thick); and, finally, small spacers placed at the four corners of the glass-epoxy 'sandwich' to ensure uniform thickness in the epoxy layer.

The immersion and fracture tests are exactly as employed in Part I. It should however be remembered that the 80°C water bath temperature is below the T_g of the SP 250 resin, whereas it was above that of the Epikote resin. This means that water diffusion rates will be considerably slower in the SP 250 resin.

Coupling agent were added as follows:

A 187 at 0.1% and 0.5% by weight.
A 1120 at 0.5% by weight.

3. CALCULATION OF COHESIVE AND ADHESIVE FRACTURE ENERGIES

This followed the same procedure as used in Part I. The function for adhesive failure, f_2, was used in all cases because in these thin specimens fracture is always very close to the interface. The fact that there exists a bi-layer (resin + glass) above the PTFE disc does, in principle, lead to complications since a single Young's modulus value cannot be used. In practice, however, the test is insensitive to resin layer thickness as long as the latter is below about 0.5 mm, which was the case for the specimens used for the major study. This is because the energy release rate is dominated by the upper sheet of glass which is both

thicker and stiffer than the resin layer. (See Fig. 12 which shows the effect on critical pressure of resin layer thickness). In calculating $2\mathcal{J}$ or θ, therefore, the resin layer is simply ignored and data on thickness and modulus for the upper glass sheet alone are fed into the formula. A small correction for the residual resin effect can be made but is much smaller than the inherent experimental scatter due to velocity variation.

It is interesting to note that the range of variation of P_c in Fig. 12 increases with the resin thickness suggesting that a wider variation in crack velocity becomes possible as the available crack path length (i.e. the resin thickness) increases.

4. RESULTS

4.1 Cohesive Failure

Figure 13 is a logarithmic plot of cohesive failure energy $2\mathcal{J}$ against immersion time at 80°C for all tests in which the failure was totally cohesive (i.e. in which no region of the fracture surface was interfacial between resin and either glass sheet). This plot is analogous to those of log. ($2\mathcal{J}_o$ or θ_o) versus time given in Part I (Figs.6,7) except that the loss function Φ remains a factor in the ordinate. The presence of Φ as a multiplier has, of course, two effects in a logarithmic plot. One is to shift the data vertically by a constant amount (neglecting plasticization effects) and the other is to spread the data into a range on account of the unknown variation of Φ with crack velocity. Referring to Fig. 13 we see that the velocity-induced spread gives a six-fold variation in $2\mathcal{J}$, but that the upper and lower limits of the spread are very well defined for the dry resin on which a large number of tests were carried out. This six-fold variation of Φ for SP 250 compares with a much greater variation of between one and two orders of magnitude found for the Epikote 828 resin, though this may well be a result of the limited crack path length in thin sandwich

specimens as already suggested. The data in Fig.13 for specimens immersed for various periods of time, although less numerous than for dry specimens, fall neatly between a constant width envelope as shown.

Over the first 300 h of immersion there is a gradual though definite linear fall in $2\mathcal{J}$ (comparable in magnitude to the fall of θ_o in the best protected specimens of Epikote resin). The appropriate k' value for this fall is some $2 \times 10^{-3}\ h^{-1}$. After 300 h, however this fall is converted into an equally definite increase in $2\mathcal{J}$ with further immersion.

These effects must be interpreted in terms of the influence of water diffusing into the resin at a temperature of 80°C. The initial fall of $2\mathcal{J}$ can be attributed to a decrease in $2\mathcal{J}_o$ at constant ϕ arising from post-cure. Although the resin was originally cured for 2 h at a much higher temperature, prolonged exposure at 80°C may well enable the curing process to continue, especially in the presence of low levels of imbibed water. (Water diffusion rates below T_g are typically two orders of magnitude lower than those above T_g, but low levels of water concentration will build up quite rapidly in the fracture zone which is within 1 mm of the access hole).

The effect of further curing upon the resin will be to tighten the molecular network and reduce $\mathcal{J}_o$ by the effect described by Lake and Thomas [1967 ; see also King and Andrews 1978].

The rise is $2\mathcal{J}$ after 300 h may be due either to the onset of hydrolysis in the network, reversing the effects of post-cure (i.e. yielding a looser network and thus an increase in $2\mathcal{J}_o$) or, alternatively to the onset of plasticization causing an increase in ϕ. In Epikote 828 resin, above its T_g, plasticization is complete within 100 h of immersion at 80°C, as reported in Part I. For SP 250, below its T_g one would expect a much longer time to equilibrium water uptake and a slow progressive plasticization effect would be expected over the range 0 to 1000 h and beyond. It is not at present possible to distinguish clearly between

these two possibilites, but we shall see presently that if the second (plasticization) explanation is adopted the adhesive results can be explained in a rational manner.

4.2 Adhesive Failure

For thin sandwich specimens, we define adhesive failure as any case in which the fracture plane passes along an interface between resin and glass, regardless of which of the two resin-glass interfaces is involved. Such interfacial fracture regions are readily recognised because of their mirror-smooth appearance.

Figure 14 shows the collected data for adhesive failure energy, θ, together with the envelope for cohesive failure $2\mathcal{J}$. These quantities are, again, plotted logarithmically against time of immersion.

There are no adhesive failures below 150 h immersion, indicating that $\theta_o > 2\mathcal{J}_o$ for dry specimens and those exposed for short periods of time. As immersion time rises beyond 150 h, however, fracture becomes progressively more adhesive in nature and beyond 600 h all failures are adhesive. It can be seen from Fig. 14 that this transition occurs as the cohesive failure envelope rises, leaving the adhesive points below its lower bound.

The behaviour of θ itself depends upon the system studied.

For soda-lime (S-L) glass as the upper plate and no coupling agent, the transition to adhesive failure takes place at 200 h and at 300 h a catastrophic fall in θ occurs. Almost exactly similar results are obtained with S-L glass even when the resin contains 0.1% of coupling agent A 187 or 0.5% of A 1120. Indeed specimens with A 1120 silane display, if anything, an earlier catastrophic loss of strength.

The catastrophic fall in θ_o in these specimens is such that no slope can be attributed to the plot of log θ versus time in this region. It appears that

as soon as water penetrates to the boundary between the resin and the upper glass plate, the loss of interfacial strength is almost total. This suggests that the interfacial bonds between SP 250 resin and the soda-lime glass employed are unstable in the presence of moisture, and that no more stable bonds are established with the addition of A 187 and A 1120 coupling agents. It is important to add that though unstable to moisture the dry bonds are not weak for if they were, adhesive rather than cohesive failure would occur in unimmersed specimens.

When identical specimens (S-L upper glas sh[illegible]) have added A 187 at the higher concentration of 0.5%, the results are quite different and θ remains high and constant for immersion times up to 1100 h, even though adhesive failure is detected after 200 h. The significance of adhesive failure at constant θ value will be discussed presently.

When both upper and lower glass sheets are of Pyrex glass, no adhesive failure is found until after 300 h of immersion. Between 300 h and 600 h, the likelihood of adhesive failure increases until all failures are adhesive in nature. For Pyrex glass specimens no significant change in the value of θ can be detected, in spite of the progressive change in failure mode from cohesive to adhesive. The value of θ remains within the range recorded for 2J at its 'low point' at 350 h. However it is important to note that θ remains constant whilst the range of 2J rises again beyond 350 h.

The addition of coupling agents to Pyrex sandwich specimens has no detectable effect, except that A 187 at 0.1% gave two low data points.
In view of the higher values recorded for identical specimens at the same immersion times, we tend to doubt the validity of these low points.

The remaining anomaly is, therefore, the observation that [illegible] remains sensibly constant for Pyrex specimens in spite of the progressive transition from cohesive

to adhesive failure which shows clearly that the interface is being weakened by exposure to moisture.

This can be completely explained if we accept that the rise in cohesive fracture energy $2\mathcal{J}$ beyond 350 h is caused by an increase in Φ , rather than $2\mathcal{J}_o$. Then we have,

$$\log 2\mathcal{J} = \log 2\mathcal{J}_o + \log \Phi(+t) \quad (12)$$

$$\log \theta = \log \theta_o(-t) + \log \Phi(+t) \quad (13)$$

In these equations the functional dependence (+t) indicates that the quantity increases with time and (-t) that it decreases with time. We expect, from Part I, a linear decrease of $\log \theta_o(-t)$ with time and we <u>observe</u> a linear increase of $\log \Phi(t)$ with time (assuming $\mathcal{J}_o$ is constant at $t > 350$ h.) It follows that $\log \theta$ will also vary linearly with time with a slope intermediate between the positive gradient of $\log \Phi$ and the negative gradient of $\log \theta_o$. It is not surprising, therefore, that $\log \theta$ should appear to be effectively independent of time (zero slope).

From equations 12, 13,

$$\log \theta_o = \log \theta - \log 2\mathcal{J} + \log 2\mathcal{J}_o \quad (14)$$

$$\log (\theta_o/2\mathcal{J}_o) = \log \theta - \log 2\mathcal{J} \quad (15)$$

thus
It is possible to replot the data as $\log (\theta_o/2\mathcal{J}_o)$ against time. Using the average value for $2\mathcal{J}$ and assuming $2\mathcal{J}_o$ to be constant, though unknown, the overall rate constant k' for bond deterioration can be obtained. The replot for SP 250/Pyrex specimens is shown as Fig. 15 , where data points for each system have been averaged in an attempt to clarify the trends.

Good straight-line behaviour is obtained with the anticipated negative slopes from which k' values can be obtained. These are as follows:-

SP 250/Pyrex/no coupling agent	k' =	$1.06.\ 10^{-3}$ h
SP 250/Pyrex/0.5% A 1120		$0.97.\ 10^{-3}$ h
SP 250/Pyrex/0.1% A 187		$0.83.\ 10^{-3}$ h

These values are similar to those found for Epikote 828 protected by 0.05% A 187, but differ in that A 187 coupling agent is more effective, at a given proportion by weight, than A 1120 in SP 250 whereas the reverse is true in Epikote.

Figure 15 inspires additional confidence, in that extrapolation to zero time of immersion gives $\theta_o > 2\gamma_o$, predicting cohesive failure for dry specimens as is observed. If the average value of $2\gamma_o$ (dry) is taken, the transition from cohesive to adhesive failure (i.e. the condition $\theta_o = 2\gamma_o$) is predicted to occur between 220 h and 280 h of immersion. These figures agree quite well with the first observed incidence of adhesive failure in the SP 250/Pyrex systems which occurred around 300 h.

In spite of the additional complexities of working with SP 250 resin, and expecially the absence of crack velocity data, it does appear that similar information can be extracted to that obtained with the low T_g resin. We do not have a value for γ_o for SP 250 and therefore no absolute values for θ_o (dry). This could be rectified by further research, however.

It was pointed out earlier that one set of data for S-L glass did not give catastrophic ($k' \sim \infty$) failure of the interface, namely the SP 250/0.5% A 187 system. Unfortunately these data are not sufficiently numerous to construct a curve such as those in Fig. 15 with any confidence. However, taking the limited information available, and using the observed immersion time for the onset of adhesive-mode failures (200 h in this system) as a means of fixing the vertical position of the curve, we obtain the result shown in Fig. 16. The Pyrex curve for 0.1% A 187 is included for comparison. However approximate this result, it is clear that a much higher proportion of A 187 is required with S-L glass than

with Pyrex glass to produce a similar degree of interfacial protection. This is, of course, consistent with the fact already noted that at 0.1% of this coupling agent the S-L interface is unstable in the presence of moisture.

5. CONCLUSIONS

The adhesion of SP 250 resin to glass is significantly affected by the nature of the glass surface, soda-lime glass adhering poorly in comparison with Pyrex (borosilicate) glass. The adhesion to soda-lime glass can be made to match that to Pyrex if sufficient couling agent (about 0.5%) is added to the resin. The adhesion to Pyrex is also enhanced by coupling agent, but less dramatically. The relative effectiveness of two coupling agents is reversed in SP 250 resin relative to Epikote 828 resin.

'Adhesion' has been successfully characterised not only by an adhesive failure energy θ, but also by a linear curve of log $(\theta_o/2\gamma_o)$ versus immersion time in water. The negative slope of this line, k', is proportional to the true chemical rate constant for the hydrolysis of interfacial bonds. The effects upon k' of glass composition, coupling agent type and coupling agent concentration have been measured over a limited range of these variables.

In the case of soda-lime glass, the resin-glass interface appears to be unstable in the presence of moisture, giving an effectively infinite value for k' once water has had time to diffuse to the interface in sufficient concentration. Addition of quite large amounts of coupling agent (e.g. 0.5% A 187) is required to give k' values for S-L glass comparable to those found with Pyrex glass in the absence of coupling agents.

The data on SP 250 resin are somewhat sparse as a consequence of the experimental problems associated with a high T_g resin. The methods described, however, appear to be capable of providing much important information even on this relatively intractable system.

Captions to Figures

Fig. 1 a) Original specimen. Circular symmetry about axis A; PTFE disc B; cast resin C; substrate block D; pressurisation port E.

b) Modified specimen. Metal washer F; glass substrate G.

Fig. 2 Cohesive or adhesive failure energy for Epikote 828/pyrex glass specimens as a function of crack velocity. Times of immersion in water at 80°C shown.

Fig. 3 As Fig. 2 but with 0.1% coupling agent A 1387 added to resin before casting.

Fig. 4 Master curve for Epikote 828/pyrex glass specimens immersed at 80°C for different times (+) dry, (○) 20 h, (×) 40 h, (□) 100 h. Broken line is master curve for the fully plasticized resin from Andrews and Stevenson (1980).

Fig. 5 As Fig. 4 but with added coupling agent A 1120. Data for 0.05% coupling agent after (□) 500 h, (+) 645 h, (◇) 1128 h; and for 0.1% after (●) 983 h, (×) 1295 h, (○) 1915 h. Full line is master curve for fully plasticized resin from Andrews and Stevenson (1980).

Fig. 6 Comprehensive data for Epikote 828/pyrex glass specimens showing dependence of $a\theta_o$ upon immersion time at 80°C for different coupling agents, different concentrations of coupling agent and different pH of environment. (pH is neutral when not stated).

(1) A 187, 0.05%, pH 13. (2) No silane. (3) A 187, 0.05%, pH 2. (4) A 187, 0.05%. (5) A 1120, 0.05%. (6) A 187, 0.1%. (7) A 1120, 0.1%. (8) A 1100, 1.0%. Broken line is value of $2\mathcal{J}_o$ and numbers on this line show when the corresponding specimen system exhibits cohesive-to-adhesive failure transition.

Fig. 7 As Fig. 6 but with all curves simultaneously shifted vertically to locate each cohesive/adhesive transition event on its appropriate curve. Ordinate now gives absolute log θ_o values.

Fig. 8 Dependence of hydrolysis rate constant on pH of environment. (○) resin without silane. (●) resin with 0.05% of A 187.

Fig. 9 Dependence of hydrolysis rate constant upon concentration for two coupling agents. (●) A 187. (○) A 1120.

Fig. 10 Thin sandwich specimen showing PTFE disc B, resin layer C, glass substrates G, PTFE spacers H.

Fig. 11 Generation of a band of points from data unresolved along the crack velocity axis. The whole band moves as θ_o varies.

Fig. 12 Effect of resin layer thickness on critical pressure for thin sandwich specimens. Boxes show spread of data points. Results are insensitive to resin thickness below 0.5 mm.

Fig. 13 All cohesive failure data ($2\mathcal{J}$) for thin sandwich specimens of SP 250/glass.

Fig. 14 All adhesive failure data (G) for thin sandwich specimens of SP 250/glass. Various coupling agents and concentrations. Soda-lime glass, (○) A 187, 0.1%; (△) A 187, 0.5%; (◍) A 1120, 0.5%. Pyrex glass, (□) No coupling agent, (×) A 1120, 0.5%, (+) A 187, 0.1%. Solid lines are envelope of cohesive data.

Fig. 15 ($\theta_o/2\mathcal{J}_o$) derived from Fig. 14 for SP 250/pyrex glass. (□) No coupling agent; (×) A 1120, 0.5%; (+) A 187, 0.1%.

Fig. 16 $\theta_o/2\mathcal{J}_o$ for SP 250 resin.
Solid line: S-L curve for A 187, 0.5%.
(×) Pyrex curve for A 187, 0.1%.

REFERENCES

Ahagon, A. and Gent, A.N., (1975), J. Polymer Sci., (Polymer Physics Ed.), 13, 1285.

Andrews, E.H., (1974), J. Materials Sci., 9, 887.

Andrews, E.H. and King, N.E., (1976), J. Materials Sci., 11, 2004.

Andrews, E.H. and Kinloch, A.J., (1973), Proc. Roy. Soc., (London) A, 332, 385.

Andrews, E.H. and Stevenson, A., (1978), J. Materials Sci., 13, 1680; (1980), J. Adhesion, 11, 17.

Comyn, J., Brewis, D.M., Shalash, R.J.A. and Tegg, J.L., (1979), 'Adhesion 3', (Ed. K.W. Allen), Appl. Sci. Publishers, p. 13.

Kaelble, D.H. and Dynes, P.J., (1977), Materials Evaluation, 35, 103.

King, N.E. and Andrews, E.H., (1978), J. Materials Sci., 13, 1291.

Lake, G.J. and Thomas, A.G., (1967), Proc. Roy. Soc. (London), A, 300, 108.

Sargent, J.P. and Ashbee, K.H.G., (1980), J. Adhesion, 11, 175.

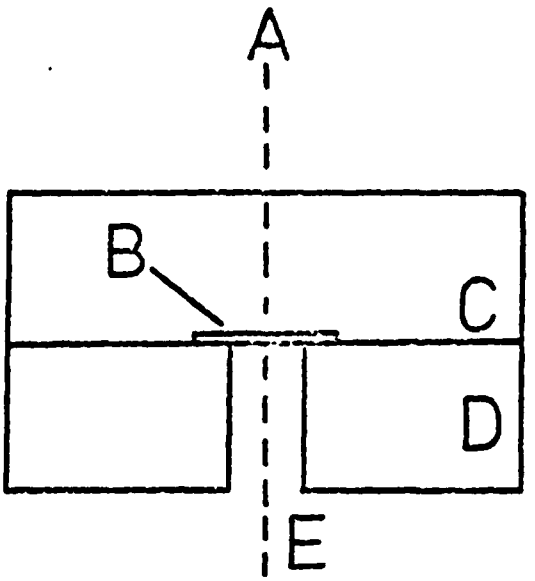

FIG. 1

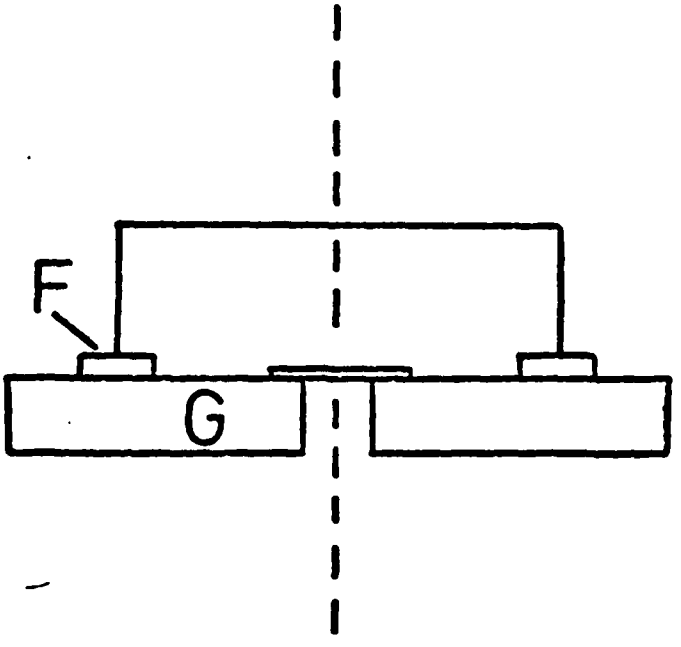

FIG. 2

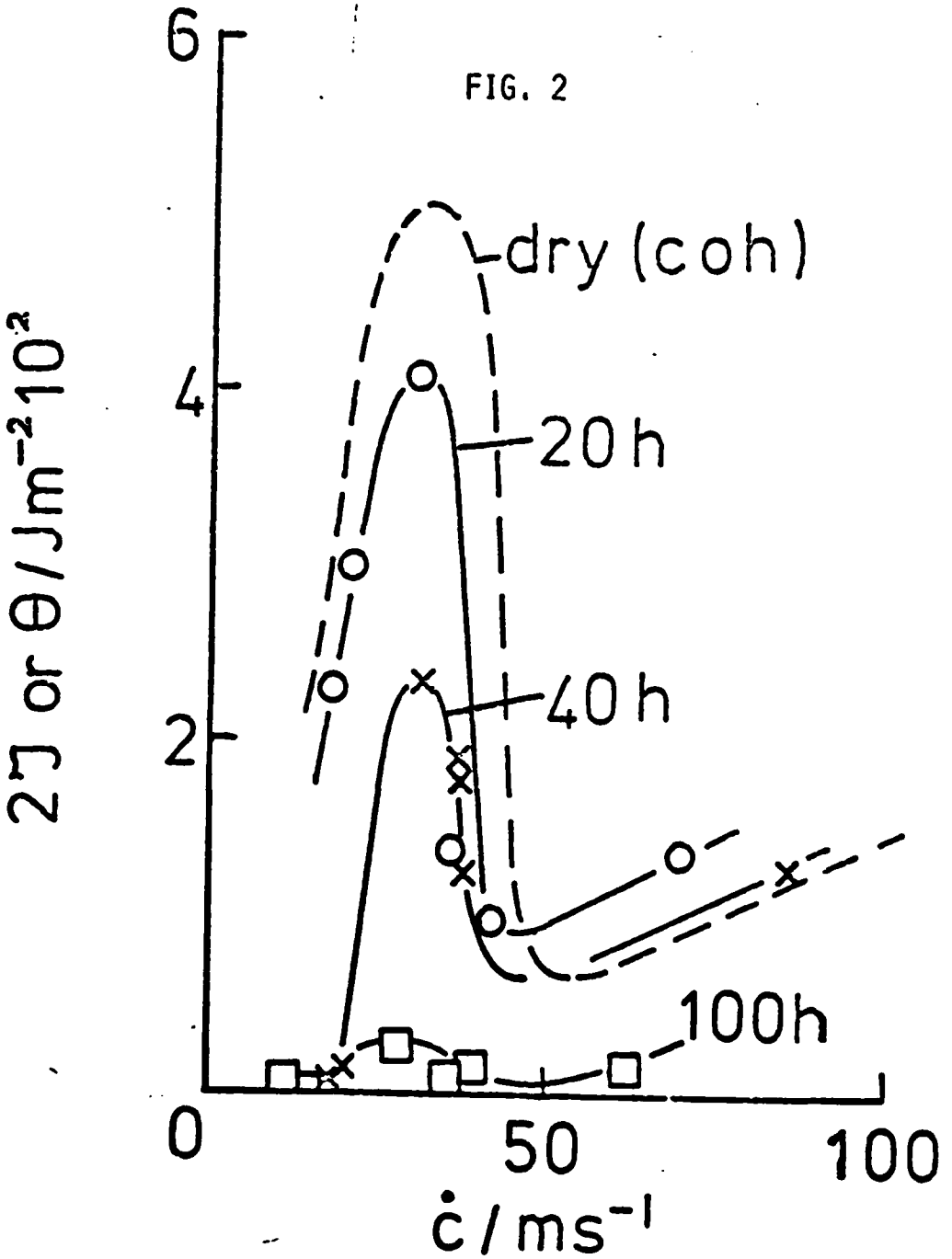
6
4
2
0
dry (coh)
20h
40h
100h
50
100
2Γ or $\theta / Jm^{-2}10^{2}$
$\dot{c} / ms^{-1}$

FIG. 3

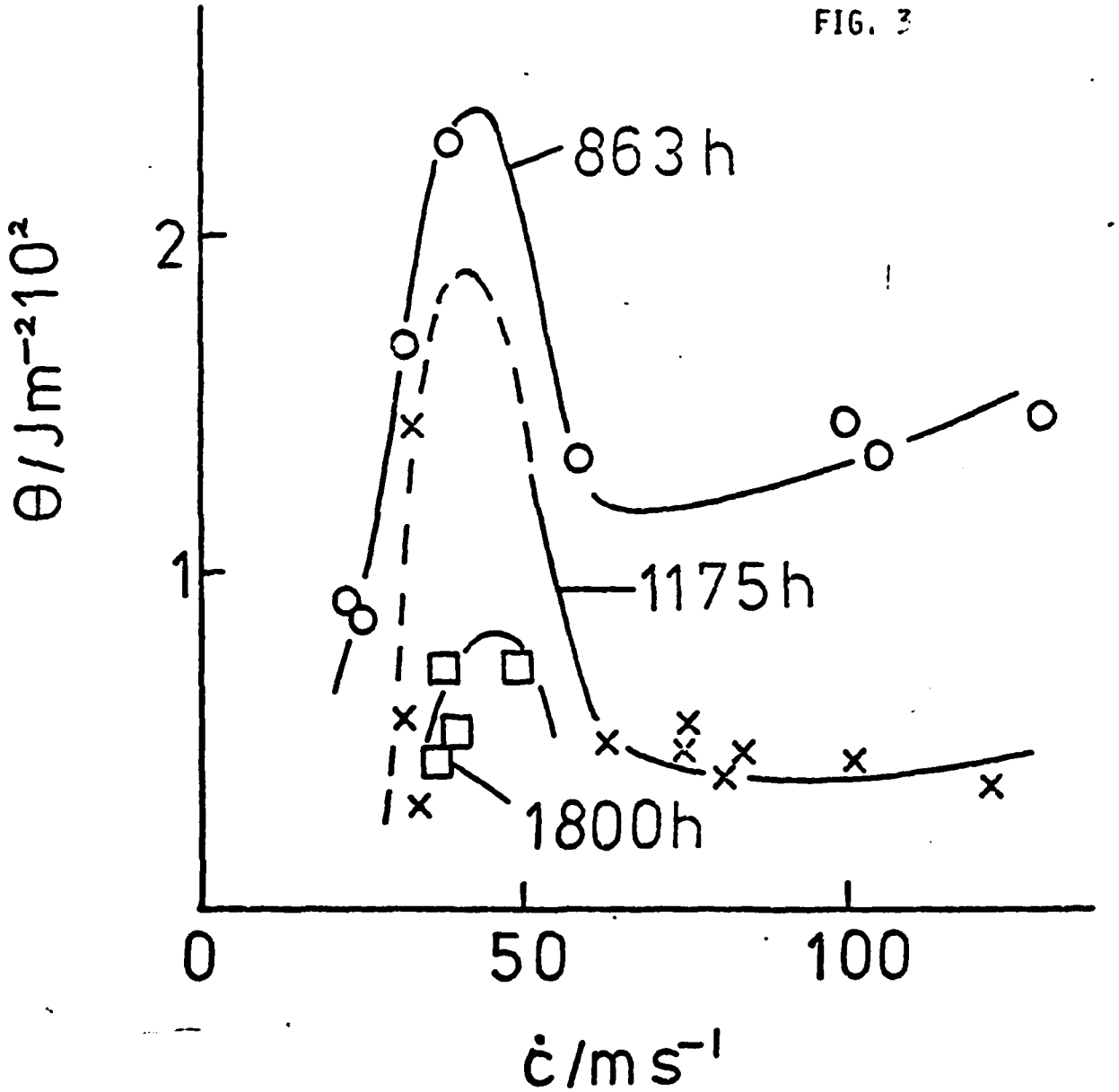

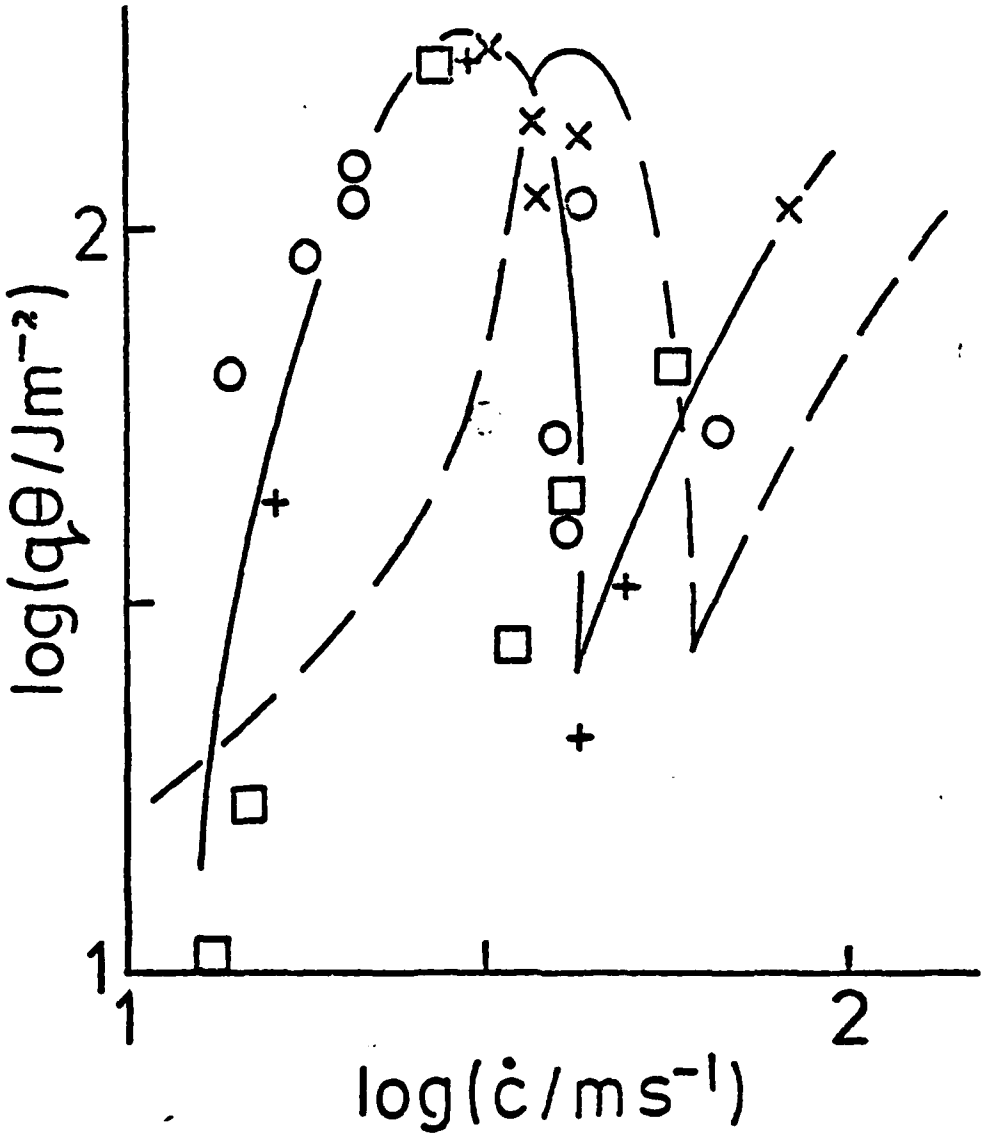

FIG. 4

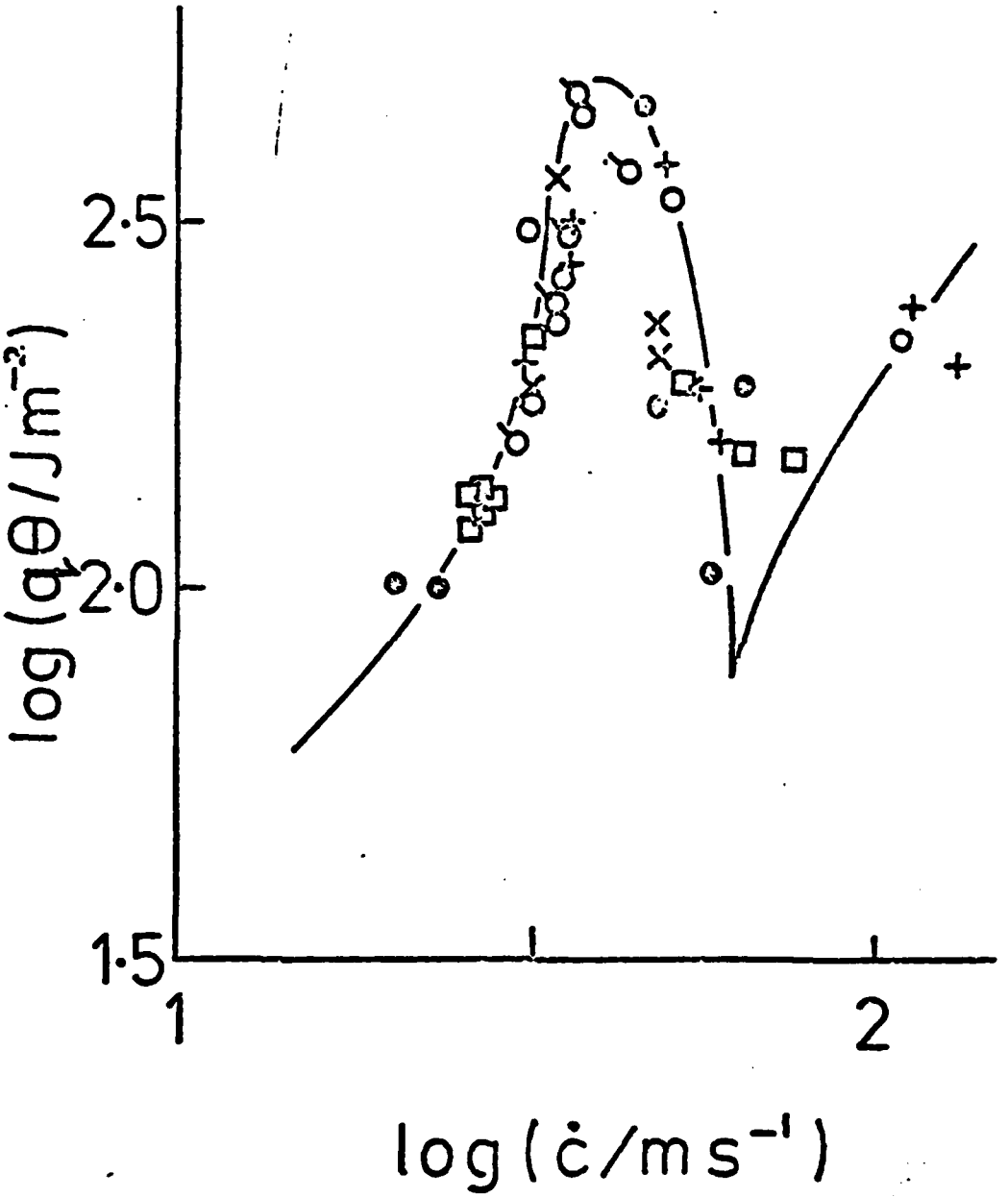

FIG. 5

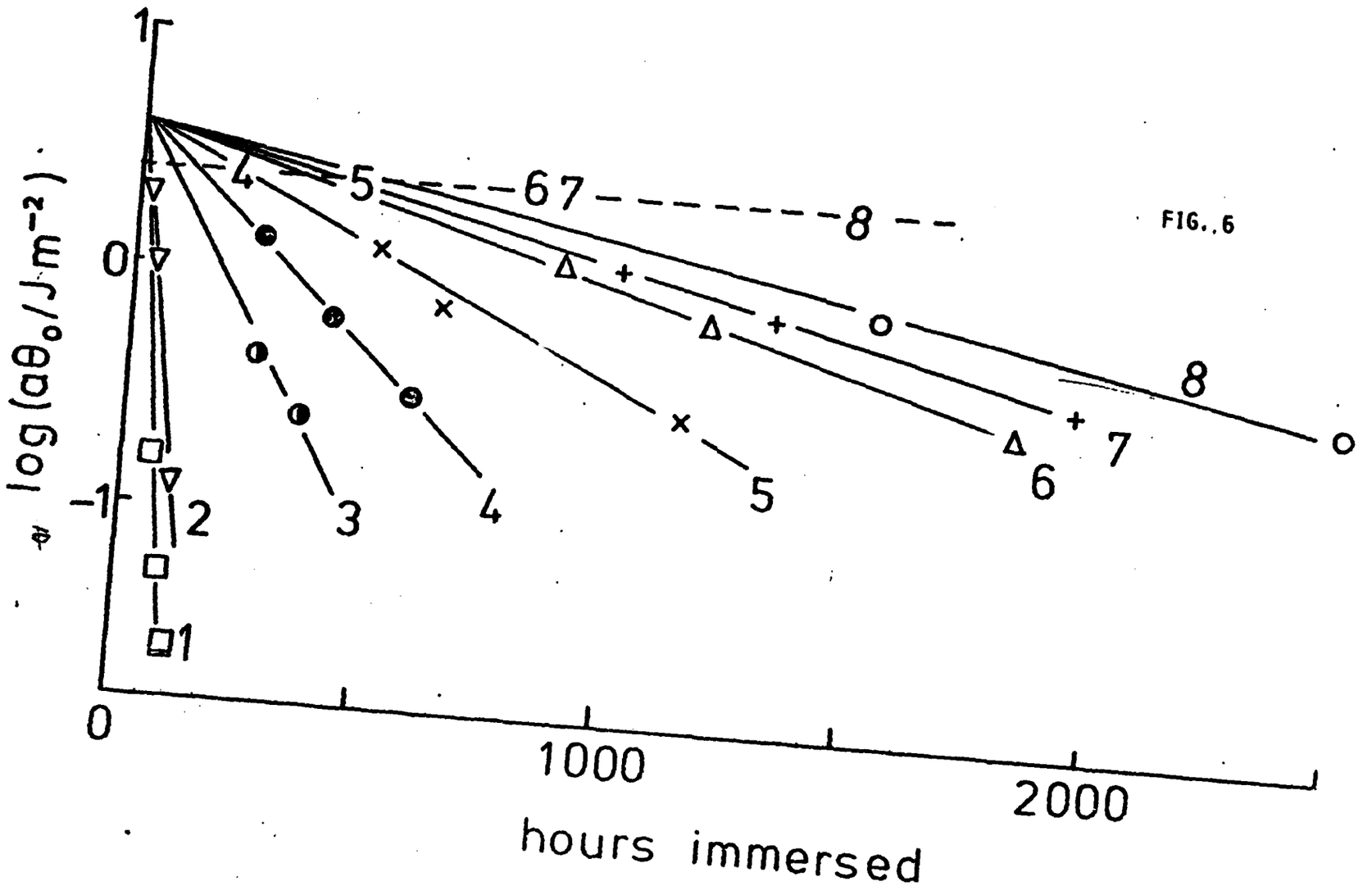

FIG. 6

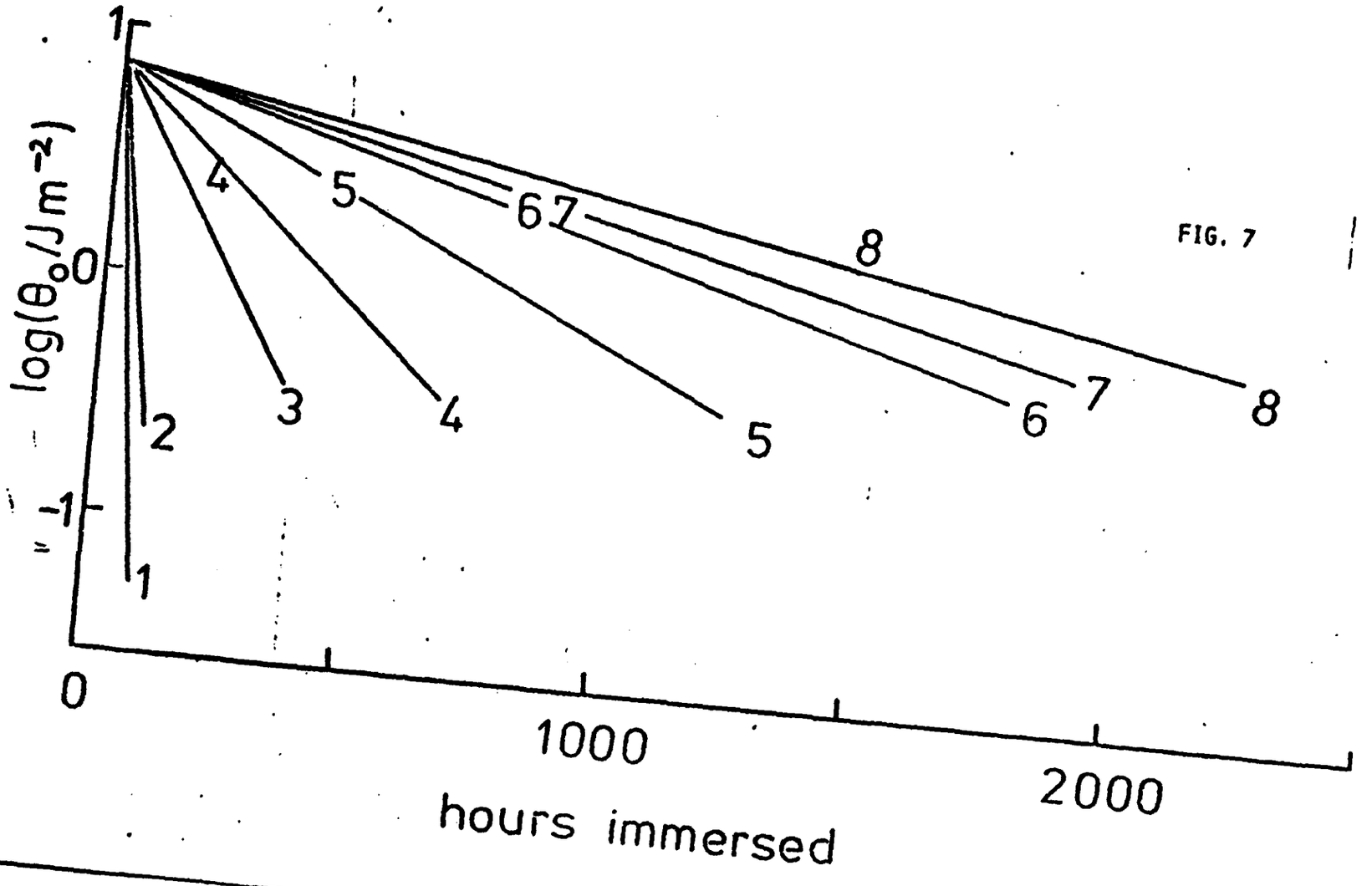

FIG. 7

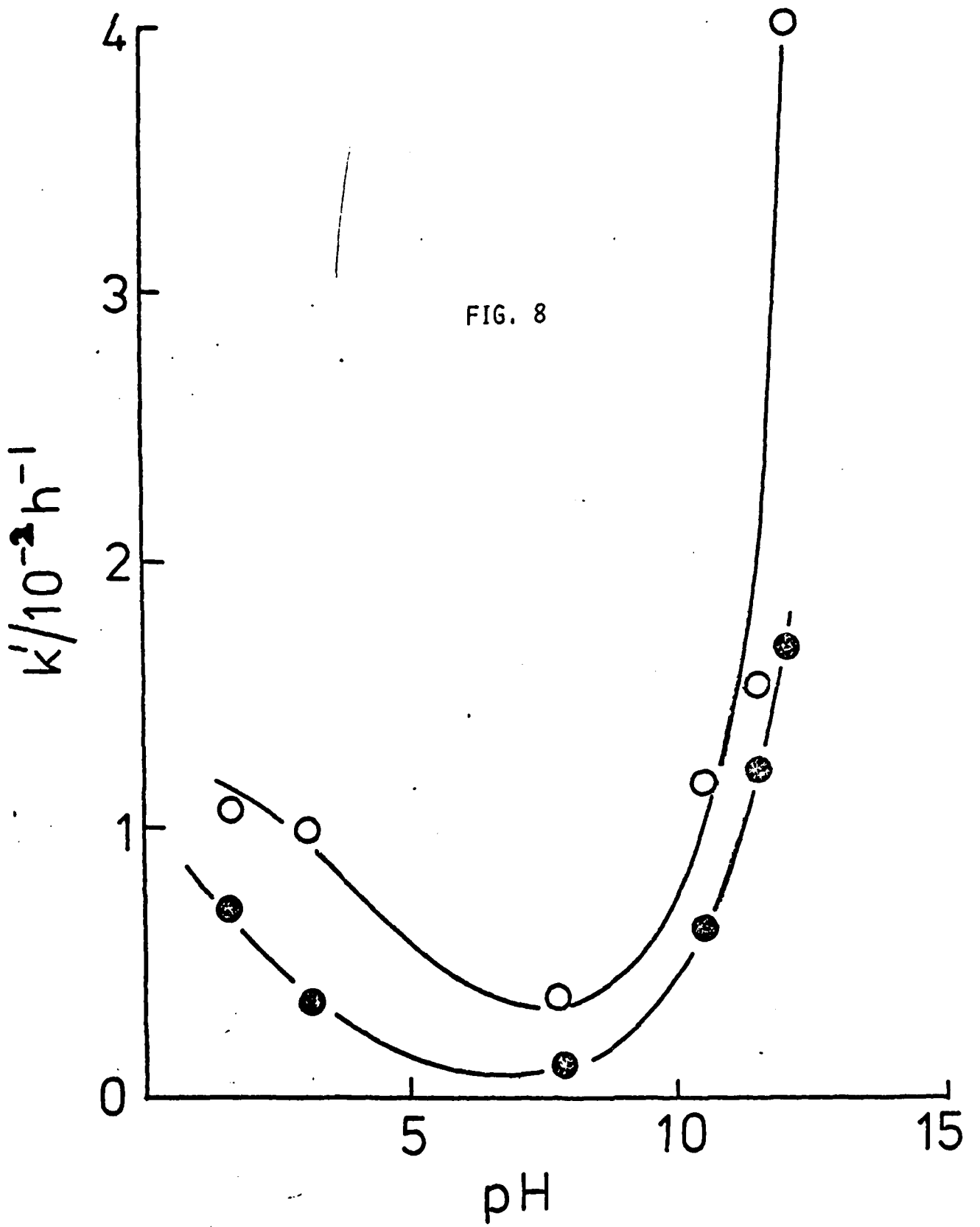

FIG. 8

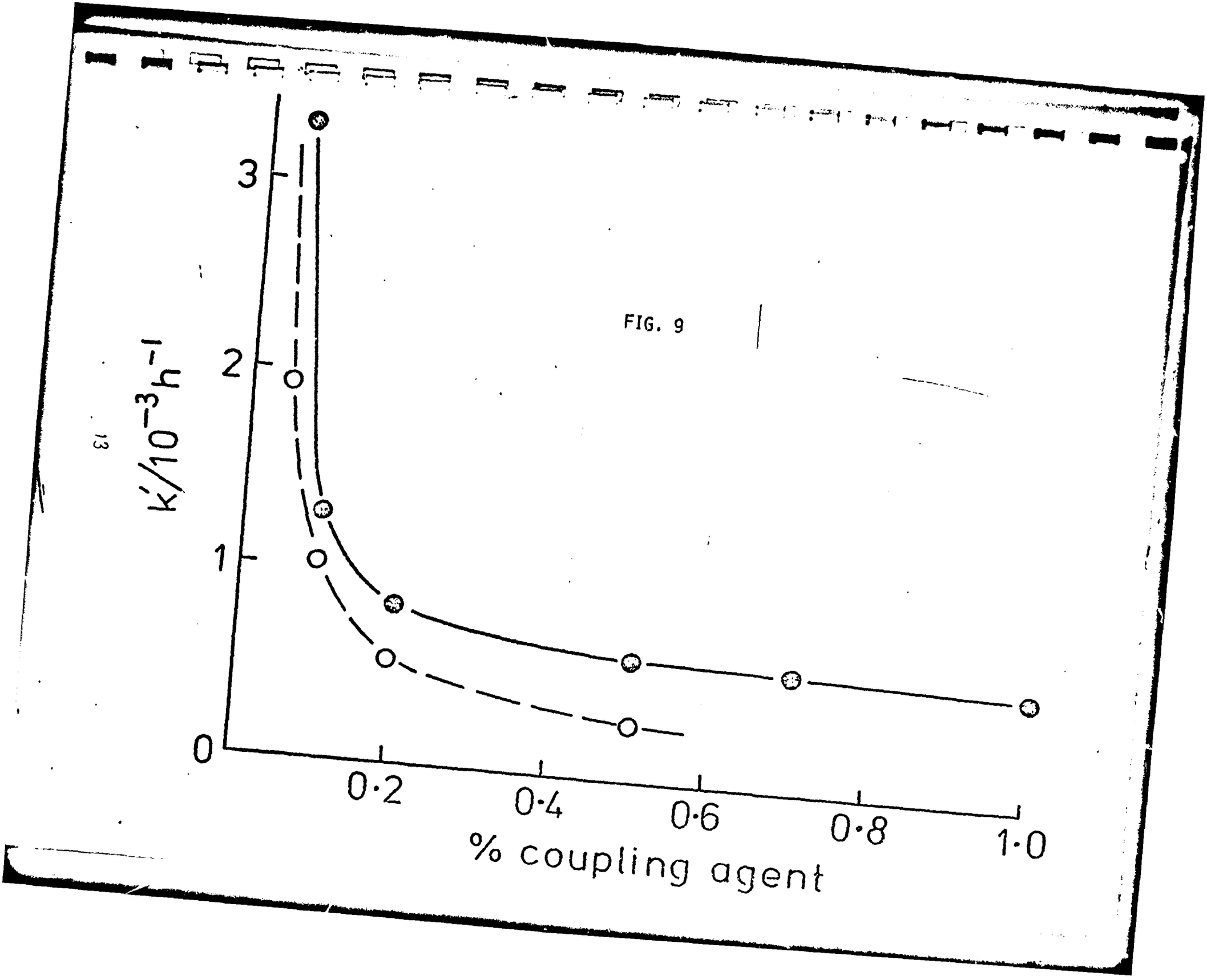

FIG. 9

FIG. 10

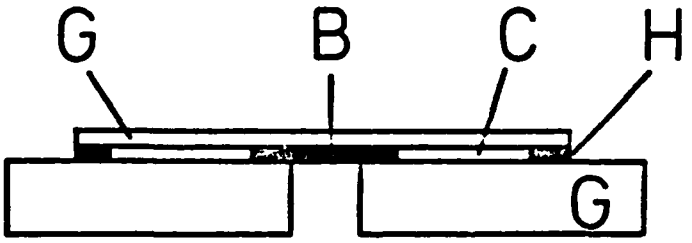

FIG. 11

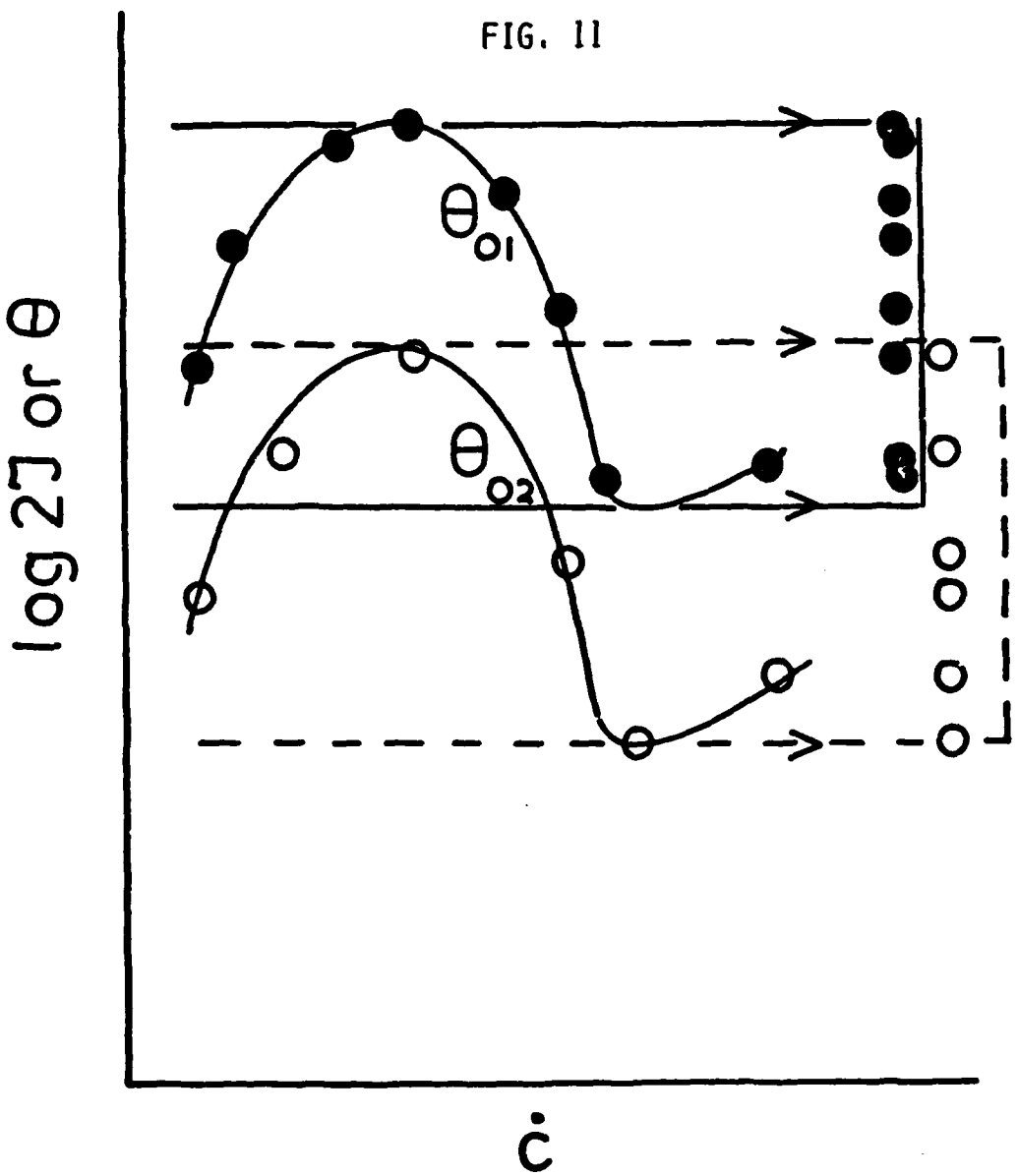

FIG. 12

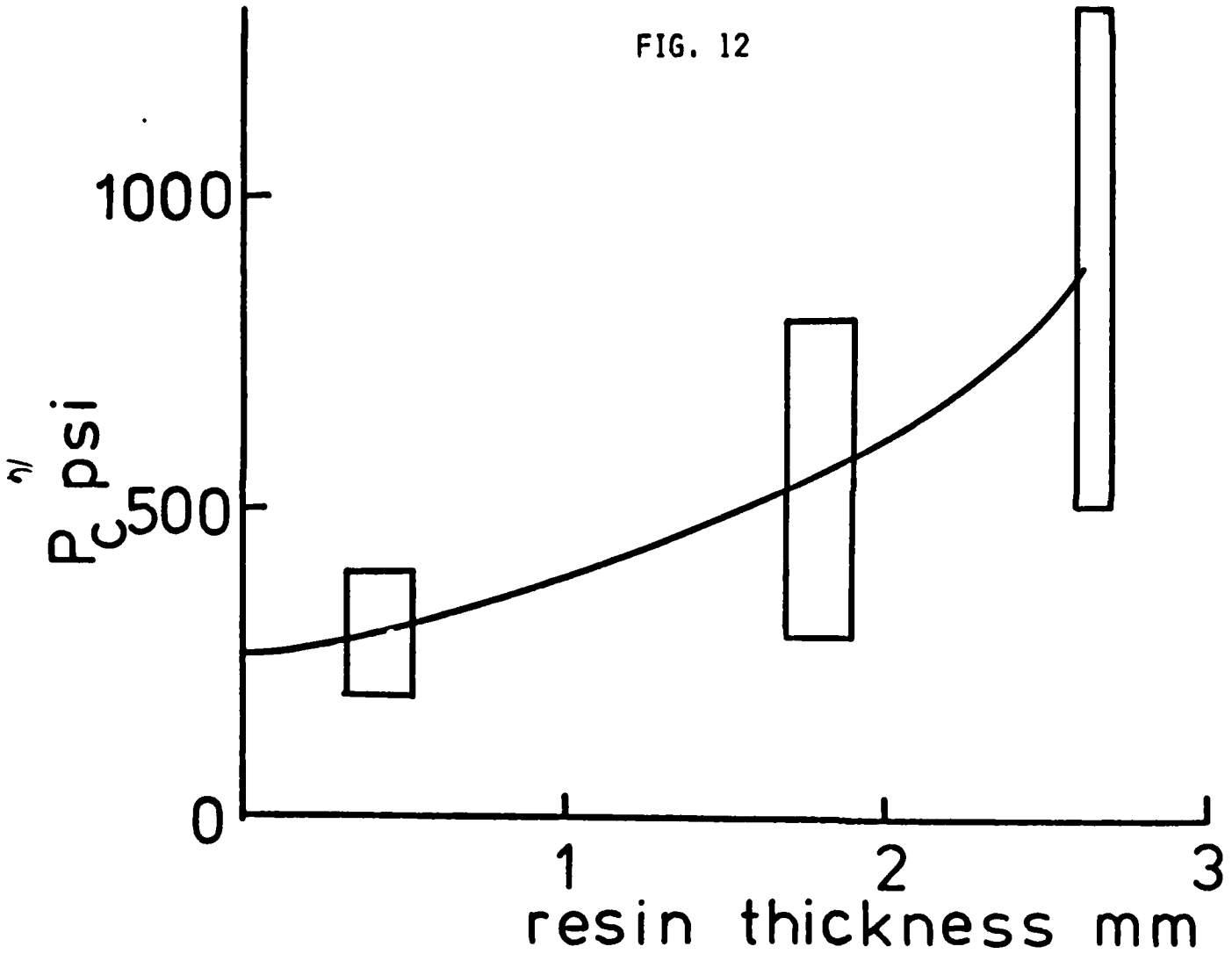

FIG. 13

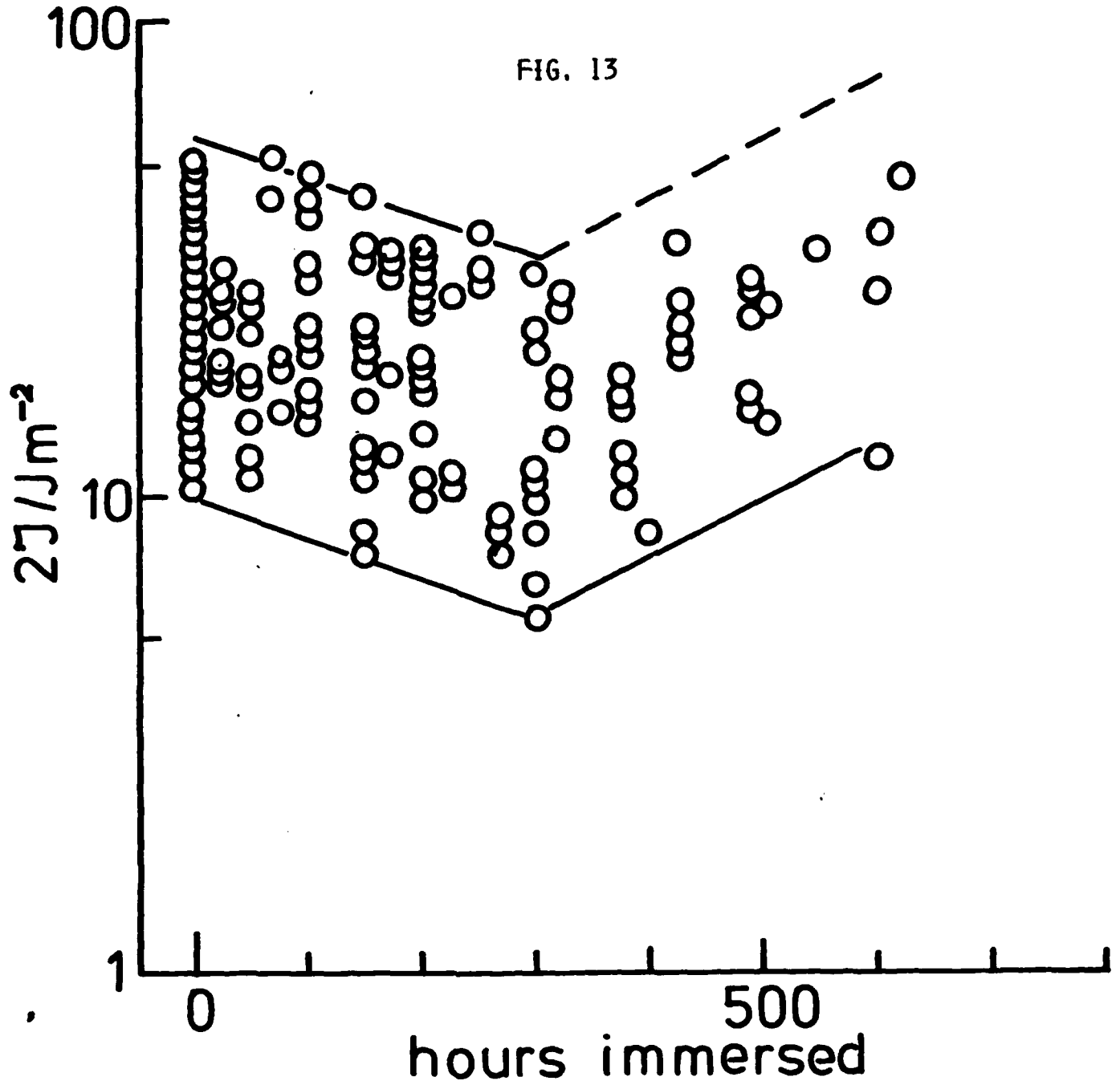

FIG. 14

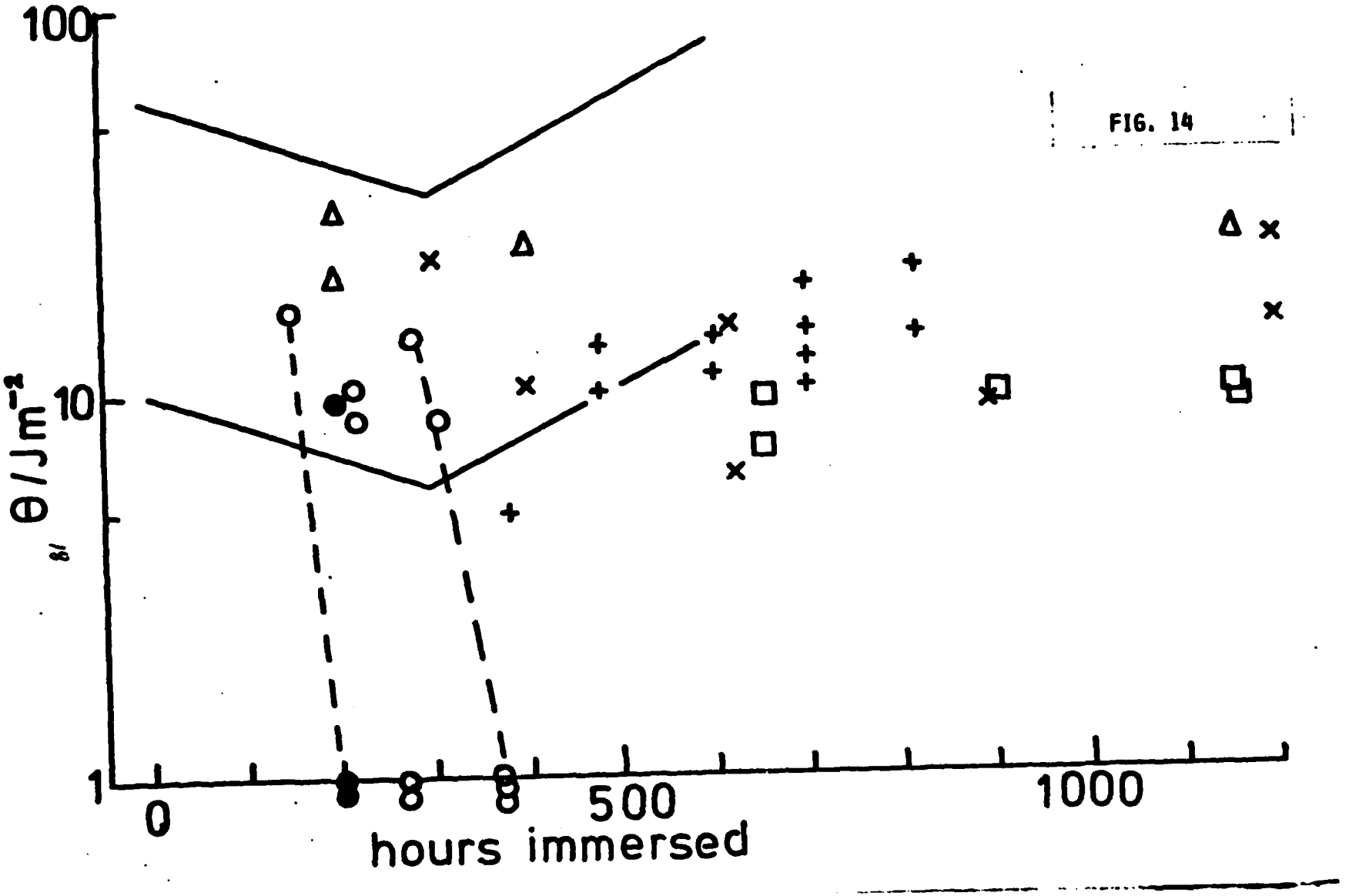

FIG. 15

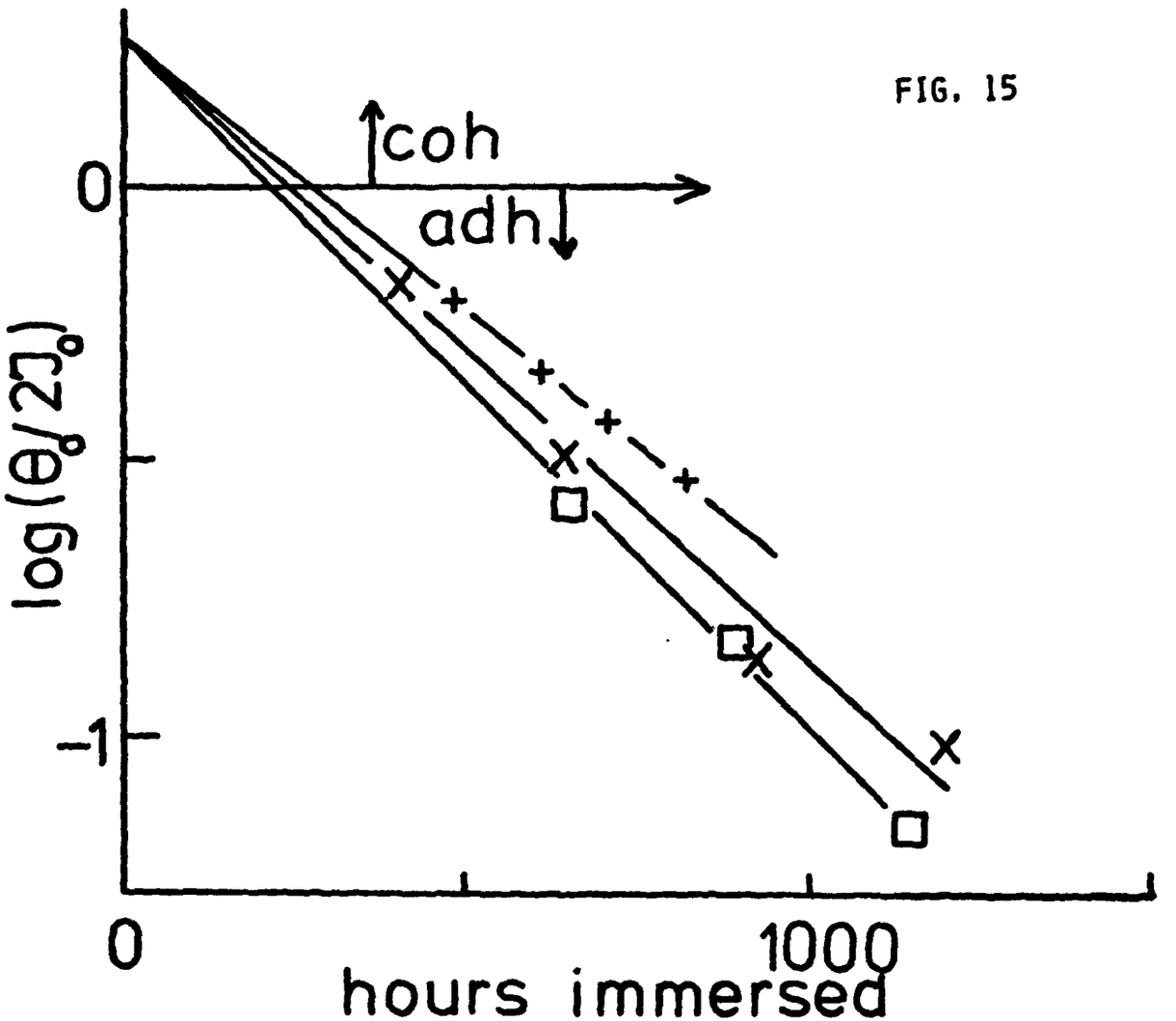

FIG. 16